Supplementary Information

Catalytic Assembled Enzyme-free Three-dimensional DNA walker and Its Sensing Application

Wei Li,[a] Lei Wang *[a] and Wei Jiang *[b]

[a] *Key Laboratory of Natural Products Chemical Biology, Ministry of Education, School of Pharmacy, Shandong University, Jinan 250012, P. R. China.*

[b] *School of Chemistry and Chemical Engineering, Shandong University, Jinan 250100, P. R. China.*

Corresponding author: Tel: +86 531 88363888. Email: wjiang@sdu.edu.cn

EXPERIMENTAL SECTION

Materials and Reagents

Oligonucleotides used in this work were synthesized by Sangon Biological Engineering Technology and Services Co., Ltd (Shanghai, China), and their sequences are listed in Table S1. Platelet-derived growth factor BB (PDGF-BB), platelet-derived growth factor AA (PDGF-AA), platelet-derived growth factor AB (PDGF-AB), human interferon-γ (IFN-γ) and human tumor necrosis factor-α (TNF-α) were obtained from the ProSpec-Tany TechnoGene Ltd (Ness Ziona, Israel). Streptavidin Magnetic Nanobeads (Streptavidin-MNBs) (350 nm diameter, 3.324×10^{11} beads/mL, 1.343 g/mL, aqueous suspension containing 0.1% bovine serum albumin (BSA)) were purchased from Bangs Laboratories Inc. (Indiana, USA). N-methyl mesoporphyrin IX (NMM) was obtained from J&K Scientific Ltd. (Beijing, China). Human serum samples were acquired from the Hospital of Shandong University (Shandong, China). Ethylenediamine tetraacetic acid disodium salt (Na_2EDTA) and other chemicals were of analytical grade and acquired from the standard reagent suppliers. All solutions were prepared using ultrapure water obtained by a Millipore Milli-Q water purification system (> 18.25 $M\Omega \cdot cm^{-1}$).

Table S1 Sequences of oligonucleotides used in this study

Name	Sequence (5′→3′)
SmallPox gene	TCA TGT GTA AGT TAC AGG ATC TAA TTG TGA
C1 for Smallpox gene	Bio-$(T)_{25}$ TCA CAA TTA GAT CCT
Swing arm for Smallpox gene	TAA CTT ACA CAT GA $(T)_{30}$ CGA CAT CTA ACC TAG CTG ACT
C1 for PDGF-BB	Bio-$(T)_{25}$ CAG GCT ACG GCA CGT AGA GCA TCA CCA TGA TCC TG
Swing arm for PDGF-BB	CAG GCT ACG GCA CGT AGA GCA TCA CCA TGA TCC TG $(T)_{30}$ CGA CAT CTA ACC TAG CTG ACT
H1	Bio-$(T)_{12}$ AGT CAG CTA GGT TAG ATG TCG CTG ACT GGG TAG GGC CGA CAT CTA ACC TAG
H2	ATG TCG GCC CTA CCC AGT CAG CGA CAT CTA ACC TAG CTG ACT GGG TAG GGC GGG TTG GG
Blocker-9	AG CTA GGTT
Blocker-10	AG CTA GGT TA
Blocker-11	AG CTA GGT TAG
Blocker-12	AG CTA GGT TAG A
Blocker-13	AG CTA GGT TAG AT
Blocker-14	AG CTA GGT TAG ATG

Note: The recognition sequences of Smallpox gene and PDGF-BB are highlighted with blur. The G-quadruples sequence is highlighted in pink.

Streptavidin-MNBs functionalization

The MNBs were functionalized with an anchorage hairpin (H1) and a ligand-captured oligonucleotide 1 (Smallpox gene-C1 or PDGF-BB-C1) through the modified literature procedure.[1,2] Briefly, 1 μL streptavidin-MNBs were washed with TTL buffer (100 mM Tris, 1 M LiCl and 0.1% Tween-20, pH=8.0) and resuspended in TE buffer (10 mM Tris and 1.0 mM Na_2EDTA, pH=9.0). Twenty microliter H1 were mixed with 20 μL ligand-captured oligonucleotide at a molar ratio of 100:1. Subsequently, this mixture was added into the MNBs suspension. The final solution was then incubated at room temperature for 2 h. The resulting products were washed twice using PBS buffer (0.15 M NaCl, 2.4 mM NaH_2PO_4 and 7.6 mM Na_2HPO_4, pH=7.4) and stored at 4 °C prior to use. The washing step should be performed in the external magnet.

Examination of the catalytic assembled DNA walker performance

The experiment was performed in TNaK buffer (20 mM Tris, 14 mM NaCl and 5 mM KCl, pH=7.5). Firstly, the ligand-captured oligonucleotide 2 (Smallpox gene-C2 or PDGF-BB-C2) and blocker oligonucleotide were heated at 95°C for 5 min in TNaK buffer and cooled slowly to 30 °C to obtain the swing arm. Then, 10 μL Smallpox gene (50 pM) or PDGF-BB (100 pM) and 10 μL swing arm were added to 10 μL DNA-functionalized MNBs suspension for 2 h at 37 °C. Next, 10 μL signal hairpins (H2) were added to the tube and kept for 2 h at 37 C°. Finally, the above products were incubated with 8 μL KCl (2 M) and 2 μL NMM for 40 min at 37 C°. Fluorescence spectra were measured with a Hitachi F-7000 fluorescence spectrometer (Hitachi, Japan). The excitation wavelength of the NMM was 399 nm with a recording emission range between 550 nm to 680 nm. The fluorescence intensity at 612 nm was used to estimate the performance of this method. The PMT detector voltage used in this method was 700 V, and the bandwidths of the excitation and emission were both 10 nm.

RESULTS

The nondenaturating PAGE experiment of the walking device

Firstly, the catalytic assembly process has been investigated in buffer. As indicated in Fig. S1A, the swing arm, H1 and H2 could be observed in line 4, line 3 and line 2. When the three

elements were mixed together, a band with slower migration rate were observed (line 1), suggesting the fact of catalytic assembly of H1 and H2. Then, the PAGE experiment of the walking process was performed. As indicated in Fig. S1B, line 2 was H2, line 3 was the swing arm, line 4 was the C1-MNB-H1 and line 5 was the Smallpox gene. The C1-MNB-H1 was stayed on the top of gel due to the presence of magnetic nanoparticle which could not migrate in the gel. Thus when the elements of walking device were mixed together, the target, the swing arm and H1 were assembled onto the nanoparticle and could not migrate in the gel (line 1).

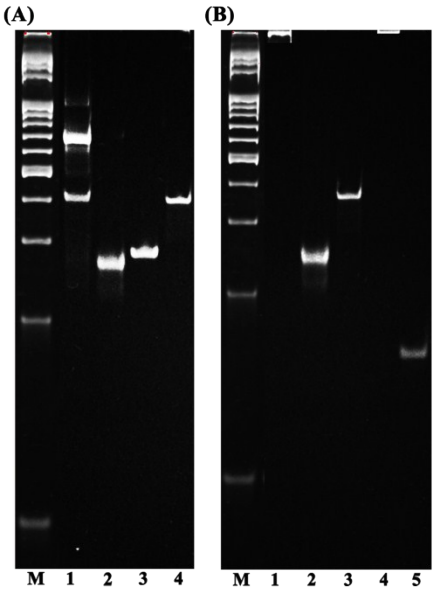

Fig. S1 (A) Nondenaturating PAGE analysis of the assembled process of the hairpins in buffer. Lane M, the DNA ladder marker; line 1, the swing arm+H1+H2; line 2, H1; line 3, H2; line 4, the swing arm. (B) Nondenaturating PAGE analysis of the walking device. Lane M, the DNA ladder marker; line 1, Smallpox gene+C1-MNB-H1+swing arm+H2; line 2, H2; line 3, the swing arm; line 4, C1-MNB-H1; line 5, Smallpox gene.

Optimization of the experimental conditions

To achieve the best sensing performance, corresponding experimental conditions were optimized. The length of the swing arm was the key factor of walking operation. So the performance of the sensing system that constructed to have varying lengths of swing arms (45, 65 or 85 nt) was investigated. As indicated in Fig. S2A, the fluorescence intensities of the device with a swing arm of 45 nt were lower than that of 65 nt and 85 nt. And similar progress curves from the operation of the walking device with 65 nt and 85 nt swing arms indicated that the two swing arms provide sufficient spatial distance to reach most anchorages on the track. Thus the swing arm of

65 nt was chosen for the sensing system. The length of Blocker also has a great effect on the sensing system. If the Blocker was too long, the combination of swing arm and H1 was difficult. The swing arm was also difficult to trigger the self-assembly of the hairpins. If the Blocker was too short, the self-assembly might carry on in the absence of target. Thus the performance of the sensing system that constructed to have varying lengths of Blockers (9, 10, 11, 12, 13, 14 nt) were evaluated. As shown in Fig. S2B, the net fluorescence intensity was reached the maximum when the length of Blocker was 11 nt, which was chosen for the walking device. Moreover, the concentration of H2 and NMM also played important roles in the sensing system. Thus the effect of H2 and NMM concentrations on the fluorescence intensities of the sensing system were evaluated, respectively. As suggested in Fig. S2C and D, the optimized H2 and NMM concentrations were 2.0×10^{-5} mol/L and 2.5×10^{-5} mol/L, respectively.

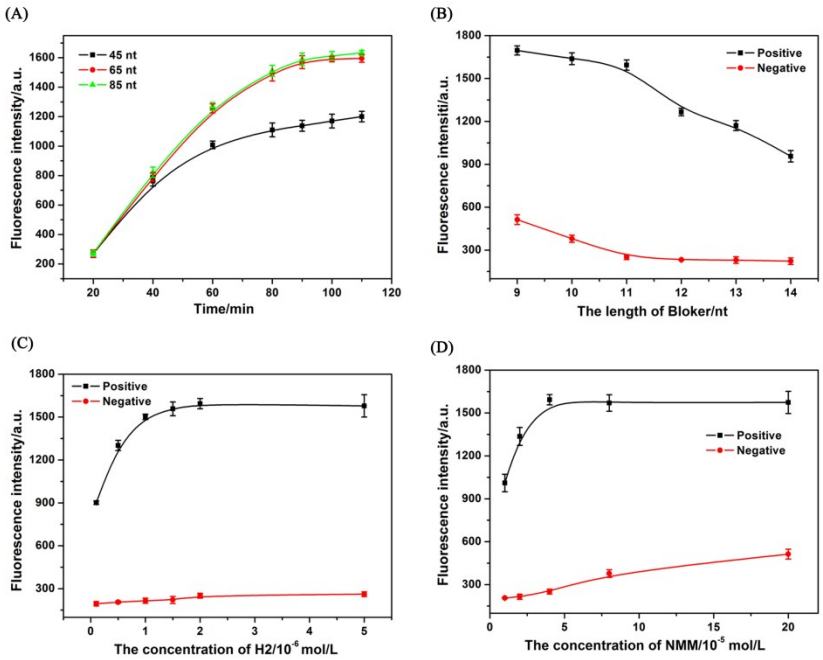

Fig. S2 (A) Progress curves of three walking devices that were constructed to have varying lengths of swing arms (45, 65 or 85 nucleotides in length). (B) Effect of the length of Blocker (9, 10, 11, 12, 13 or 14 nucleotides in length) on the fluorescence intensities of the sensing system. (C) Effect of the H2 concentration on the fluorescence intensities of the sensing system. (D) Effect of the NMM concentration on the fluorescence intensities of the sensing system.

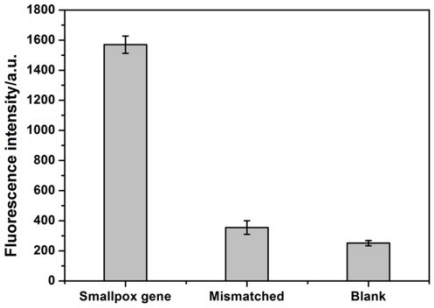

Fig. S3 Comparison of the fluorescence intensity in the presence of Smallpox gene and the mismatched sequence.

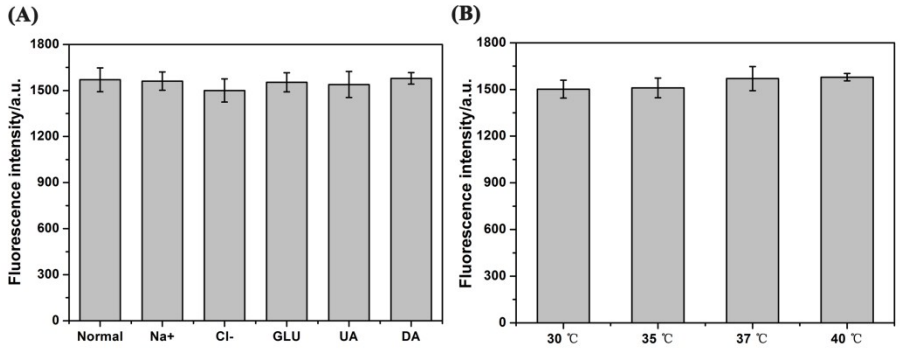

Fig. S4 (A) Effects of the matrix components on the fluorescence intensities, the concentration of Na+, Cl-, CLU, UA and DA were 146 mM, 180 μM, 6.11 mM, 420 μM and 0.8 nM, respectively. (B) Effects of the system temperature on the fluorescence intensities.

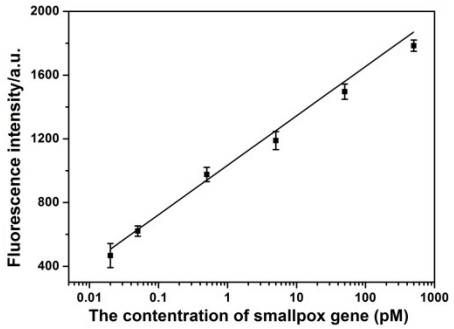

Fig. S5 Linear relationship between the fluorescence intensity and Smallpox gene concentration that spiking in human serum. The linear relationship could be described as F = 1041.4 + 293.1 lgC with a correlation coefficient of R = 0.995.

Table S2 Recoveries of Smallpox detection that spiking with human serum

Sample	Added (pM)	Detected (pM)[a]	Recovery (%)	RSD (%)
1	500	498	99.6%	5.7%
2	5	5.11	102.2%	6.7%
3	0.05	0.0523	104.6%	3.9%

[a] The average value for three measurement results.

Typical progress curve of the protein activated enzyme-free walking device

As indicated in Fig. S6, upon the addition of PDGF-BB, the catalytic assembly of H1 and H2 gave rise to the fluorescence. The progress curve suggested the fact that the walking device operated in three phases. Once activated, the walking device produced G-quadureplx at an original linear rate for about 60 min, which was phase 1. Nucleic acid recognition and hybridization positioned the swing arm in close to H1 on the track, and the catalytic assembly followed steady state kinetics. After a large amount of H1 was assembled with H2, fewer H1 were available for the swing arm. Thus the walker operation became slower (phase 2, 60-90 min). Finally, when no H1 was accessible on the track, the operation of walking device completed and the fluorescence reached the plateau (phase 3, 90-110 min). The progress curve activated by the protein target was in corresponding to that triggered by the nucleic acid target.

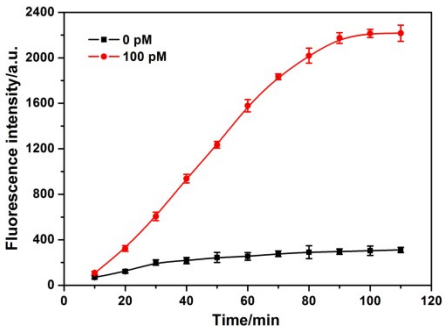

Fig. S6 Typical progress curve generated by the protein target.

Reference

1. W. Li, W. Jiang, S. Dai and L. Wang, Anal. Chem., 2016, 88, 1578-1584.

2. S. Dai, Q. Xue, J. Zhu, Y. Ding, W. Jiang, L. Wang, Biosens. Bioelectron., 2014, 51, 421-425.